ACS OMEGA

Open Access

http://pubs.acs.org/journal/acsodf

Article

Mechanistic Study of $B(C_6F_5)_3$-Catalyzed Transfer Hydrogenation of Aldehydes/Ketones with $PhSiH_3$ and Stoichiometric Water

Yunqing He,*,∇ Zhiguo Wen, Wanli Nie,*,∇ and Li Yang

Cite This: *ACS Omega* 2024, 9, 341−350

Read Online

ACCESS | Metrics & More | Article Recommendations | Supporting Information

ABSTRACT: A DFT study was performed on the mechanisms of $B(C_6F_5)_3$-catalyzed transfer hydrogenation of aldehydes/ketones, using $PhSiH_3$ and stoichiometric water. Path B2 includes a stepwise Piers S_N2-Si process, H^- transfer, and hydrolysis desilylation of siloxane, in which the hydrolysis desilylation step is rate-determining. Path C1 is first determined, involving a $B(C_6F_5)_3$-catalyzed concerted addition step of $2H_2O$ to carbonyl generating $R^1R^2C(OH)_2$, a subsequent S_N2-Si dehydroxylation step of $R^1R^2C(OH)_2$ giving $R^1R^2C{=}OH^+$ and $(C_6F_5)_3B{-}H^-$, and final H^- transfer producing the respective alcohol R^1R^2CHOH. A $B(C_6F_5)_3$-catalyzed H_2 generation process (Path H0) is determined. Path B2 is the only mechanism for the stepwise method. Using a one-time one-pot feeding method, alkyl/aryl aldehydes, dialkyl ketones, and alkyl aryl ketones (**1a−g**) can be reduced into alcohols chemoselectively and effectively at room temperature. More than 1 equiv of water over substrates is necessary. Herein, Path C1 is the dominant transfer hydrogenation pathway, and the H_2 generation is efficiently inhibited, by the competitive advantage of Path C1 and initial dominant existence of the complexes IM0 and IM1-x. The diaryl ketones (**1h**,**1i**) cannot be efficiently reduced into the respective alcohols using the one-time feeding one-pot method. The barriers of C-TS1-h/i are obviously higher than those of C-TS1-a−g, attributed to the electron-donating and space effects of the two aryls on carbonyl C. The possible Paths B2 and C1 of transfer hydrogenation have no competitive advantage with Path H0. The DFT results are consistent with the experiments.

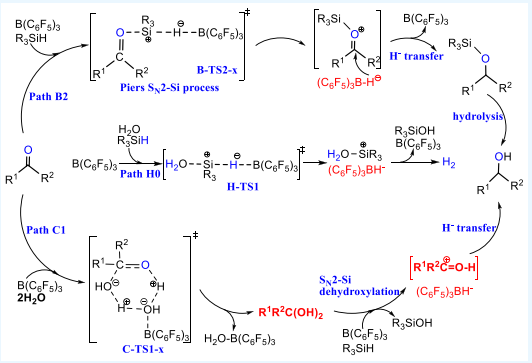

1. INTRODUCTION

Reduction of carbonyl compounds remains a significant research field of organic chemistry,[1] and precious and transition metals such as Ni, Pd, Ru, Co, Fe, and others have often been used in the relevant catalytic systems.[2−8] Since the Stephan group reported the paradigm of metal-free reversible activation hydrogen in 2006, frustrated Lewis pair (FLP) chemistry has attracted great attention and been applied in a growing body of chemical problems,[9−23] in which Lewis acid (LA) boranes, especially $(C_6F_5)_3B$-based ones, can effectively activate H_2 or Si−H and have frequently been used in the catalytic reduction of imines, enamines, alkenes, alkynes, and others. Nevertheless, catalytic FLP reduction of carbonyls has been a longstanding problem for strong B−O bonds[23−27] until 2014, when the Stephan and Ashley groups reported their FLP-based carbonyl reduction, using weakly coordinating solvents ether and 1,4-dioxane, respectively, in which $B(C_6F_5)_3$ and ether behave as FLPs to activate H_2 and effect the reduction.[28−32] It is *a priori* assumed that any $B(C_6F_5)_3$-involving reaction system requires strictly anhydrous conditions.[20−23] Generally $B(C_6F_5)_3$-catalyzed aldehyde/ketone reduction with hydrosilanes is performed using a stepwise method, first siloxane is generated by hydrosilylation of carbonyl in anhydrous systems and then hydrolytic desilylation of siloxane is performed to produce the final alcohol. Piers, Sakata, et al. proposed a S_N2-Si silane activation mechanism (Scheme 1, a) rather than carbonyl activation (Scheme 1, b).[33−36]

For systems involving water, the coordination of water to $B(C_6F_5)_3$ and irreversible O−H activation have usually been the main recent challenges, because water may prevent substrates from interacting with $B(C_6F_5)_3$ by forming the

Scheme 1. Traditional Mechanisms of $B(C_6F_5)_3$-Catalyzed Aldehyde/Ketone Reduction with Hydrosilanes

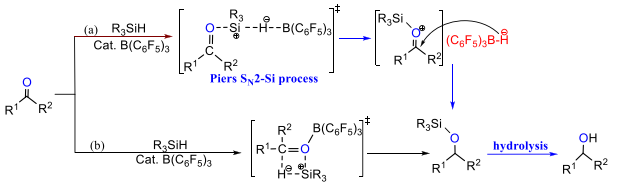

Received: July 24, 2023
Revised: October 24, 2023
Accepted: November 27, 2023
Published: December 18, 2023

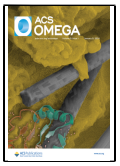

complex $(C_6F_5)_3B{-}OH_2$, and deprotonation or protodeboronation of $(C_6F_5)_3B{-}OH_2$ yields inactive hydroxy species (Scheme 2).[20−23]

Scheme 2. Deprotonation or Protodeboronation of $(C_6F_5)_3B$-OH_2 Yielding Inactive Hydroxy Species

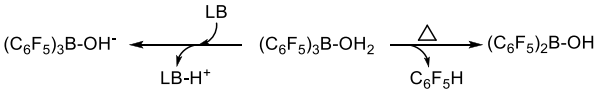

Predominantly, avoiding moderate to strong Brønsted bases to prevent irreversible deprotonation of $LA{-}OH_2$ or altering electronic and steric factors of the active LA center to reduce the coordination propensity of water to LA, recently significant progress has been made to overcome water intolerance in FLP systems.[23] Ashley and Stephan's groups reported $B(C_6F_5)_3$-catalyzed aldehyde hydrogenation in reagent grade polar solvents,[28−32] Soós and co-workers developed a highly water tolerant boron/nitrogen-centered FLP,[37,38] and Ingleson and Chang's groups reported successful one-pot borane-catalyzed reductive amination or hydrosilylation.[39−41] $B(C_6F_5)_3$ was generally supposed to be water-tolerant and a small amount of water did not affect its catalysis activity, for the deprotonation of $(C_6F_5)_3B{-}OH_2$ was reversible in these systems.

Nowadays the mechanism of borane-based FLP chemistry under water-containing conditions is of great concern. Ingleson et al.,[39−41] Wei et al.,[42] and Broadbelt et al.[43−45] have recently reported mechanism studies concerning borane-catalyzed reductive amination (containing 1 equiv of water as an intermediate), and a $B(C_6F_5)_3$-catalyzed 1,2-epoxyoctane alcoholysis ring-opening reaction in undried alcohol, water may participate reactions and influence the regioselectivity. In recent years, our group performed a series study on $B(C_6F_5)_3$-catalyzed reductive amination, imine reduction, and carbonyl compound reduction, containing stoichiometric water in systems.[46−48] When all the reactants and catalysts were added into the system simultaneously, for imine reduction, the newly determined $(C_6F_5)_3B{-}OH_2$-induced mechanisms (Scheme 3) involving intermediate $(C_6F_5)_3B{-}OH^-$ are

Scheme 3. Recently Determined $(C_6F_5)_3B$-OH_2-Induced Mechanisms for Imine Reduction Using Hydrosilylation under Stoichiometric Water Conditions

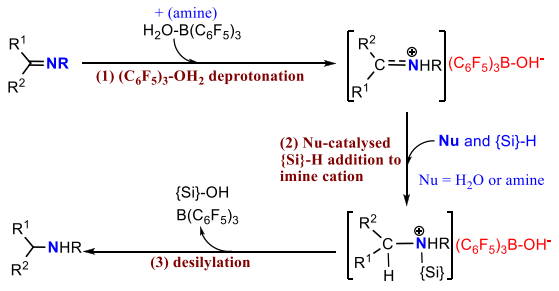

competitive with Ingleson's conventional path, and their competitive behaviors result in excess water or added/produced amine playing as on−off species for chemoselectivity of imine reduction.[47]

Recently, our group confirmed that, at room temperature, a series of carbonyl compounds (involving alkyl/aryl aldehydes, dialkyl ketones, and alkyl aryl ketones) can be reduced into alcohols chemoselectively and effectively, catalyzed by $B(C_6F_5)_3$, using hydrosilanes ($PhSiH_3$, Ph_2SiH_2, and Et_3SiH) as reducing agents, under 2−3 equiv water over substrates or even under water conditions (Scheme 4); more than 1 equiv of

Scheme 4. $B(C_6F_5)_3$-Catalyzed Aldehyde/Ketone Reduction under Stoichiometric Water or under Water Conditions[48]

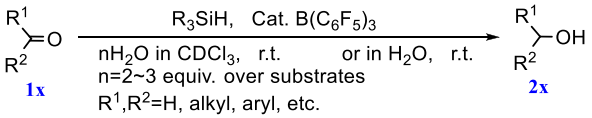

water over the substrate is necessary; while diaryl ketones can not be efficiently reduced into the respective alcohols under the same condition.[48] Attributed to the dominant existence of the ternary complexes $(C_6F_5)_3B{-}O(H){-}H{-}OH_2$ and $(C_6F_5)_3B{-}O(H){-}H{-}O{=}CR^1R^2$, the free borane catalyzed side reaction between hydridosilane and water producing H_2 was inhibited, which makes hydridosilane able to be used as reductant, in the presence of water.[48] However, the in-depth mechanism has not been disclosed. Can the $(C_6F_5)_3B{-}OH_2$-induced mechanisms of imine reduction be simply assumed to be appropriate for carbonyl compound reduction, under stoichiometric water conditions?

Interestingly, it is verified that the proton cannot transfer directly from $(C_6F_5)_3B{-}OH_2$ to carbonyl O (Scheme 5), by

Scheme 5. Direct H^+ Transfer from $(C_6F_5)_3B$-OH_2 to Carbonyl O Is Impossible

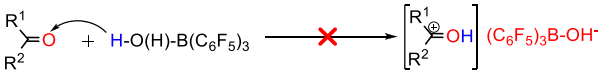

potential surface scanning using PhCHO as a model (Figure S1), which is attributed to the weaker basicity of carbonyl in comparison to imine. This implies that the mechanism of aldehyde/ketone reduction in stoichiometric water systems must fundamentally differ from that of imine.

This work presents an in-depth density functional theory (DFT) investigation on the mechanisms of $B(C_6F_5)_3$-catalyzed aldehyde/ketone ($R^1R^2C{=}O$) reduction into alcohols, using $PhSiH_3$ (as a model of hydrosilanes) and stoichiometric H_2O. If not otherwise specified, all the reactants and catalysts were added into the systems at the beginning (one-time feeding one-pot method). The aldehydes/ketones (**1x** = **1a**−**i**) used in computations are shown in Scheme 6; **1a**−**g** and **1h**/**i** were successful and failure examples given in ref 48, respectively.

The pathways (Paths A, B1, B2, C1 and C2) of transfer hydrogenation of aldehydes/ketones using $PhSiH_3$ (Scheme 7), the H_2 generation process (Path H0, see Scheme 8), and

Scheme 6. Aldehydes/Ketones 1x (1a−i) Used in Computations

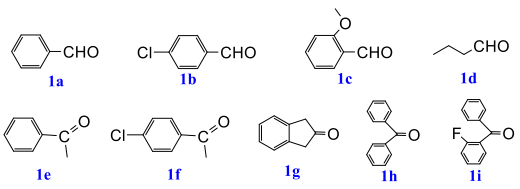

https://doi.org/10.1021/acsomega.3c05388
ACS Omega 2024, 9, 341−350

Scheme 7. Pathways of the Transfer Hydrogenation of Aldehydes/Ketones Using $PhSiH_3$

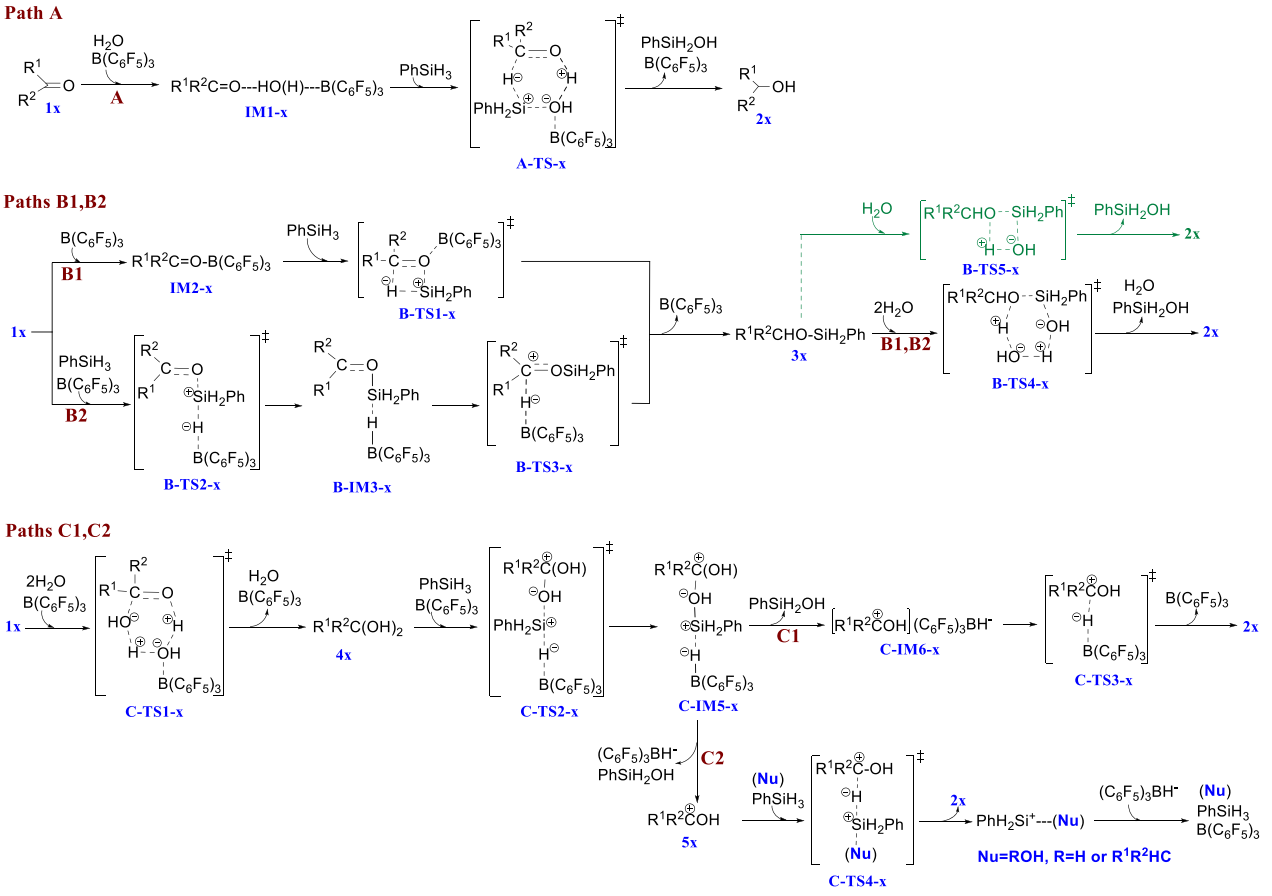

Scheme 8. Pathways of H_2 Generation and the Hydrogenation of Aldehydes/Ketones

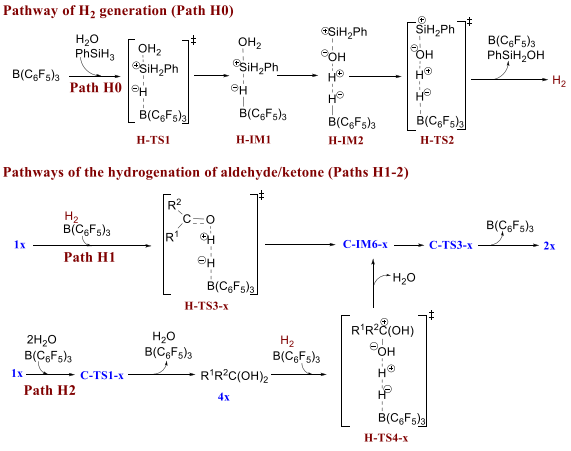

the hydrogenation of aldehydes/ketones (Paths H1 and H2, see Scheme 8) are considered. Path A is a concerted addition of hydrosilane and water to carbonyl with the catalysis of $B(C_6F_5)_3$. Paths B1 and B2 are based on the traditional carbonyl activation mechanism and the Piers S_N2-Si silane activation mechanism, respectively. Path B1 includes simple hydrosilane addition to $B(C_6F_5)_3$-activated carbonyl giving silyl ethers (**3x**) and a subsequent hydrolysis desilylation step; Path B2 includes a stepwise Piers S_N2-Si process and H^- transfer generating silyl ethers (**3x**) and a final hydrolysis desilylation step common to Path B1. Paths C1 and C2 are newly proposed ones; first $R^1R^2C(OH)_2$ (**4x**) is generated by a $B(C_6F_5)_3$-catalyzed concerted addition process of $2H_2O$ to carbonyl, subsequently protonated cations $R^1R^2C{=}OH^+$ (**5x**) and $(C_6F_5)_3B{-}H^-$ are given by a S_N2-Si dehydroxylation step of $R^1R^2C(OH)_2$, and finally H^- transfer produces the respective alcohol R^1R^2CHOH. In Path H0, a S_N2 process gives $B(C_6F_5)H^-$ and $PhH_2Si^+{-}OH_2$ first, and then H_2 is produced. In Paths H1 and H2, $B(C_6F_5)_3$ and aldehydes/ketones or geminal diols (**4x**) behave as FLPs to activate H_2.

2. COMPUTATIONAL DETAILS

Optimization and frequency analyses of stationary points and intrinsic reaction coordinate (IRC)[49−51] calculations were performed in the gas phase at the B3LYP/6-311G(d,p) level to confirm the geometries of reactants, products, transition states, and intermediates and their relationships. Solvent effect correction was performed at the B3LYP/6-311G(d,p) level with Grimme's D3 BJ dispersion correction[52] using the SMD model[53−55] in chloroform. Single-point energies in solvent were combined with the thermodynamic corrections in the gas phase to obtain the Gibbs free energies in solvent. 1 M standard state corrections were performed to adjust the results from the SMD model at 1 atm. Some potential surface scanning was performed to verify that there was no corresponding transition state. We acknowledge the successful performance of the same or similar calculation levels for similar systems.[46−48] All the computations were performed using the Gaussian 16 program package.[56]

https://doi.org/10.1021/acsomega.3c05388
ACS Omega 2024, 9, 341−350

3. RESULTS AND DISCUSSION

Taking PhCHO as an example of aldehydes/ketones, it is determined that, in reaction systems containing stoichiometric water, ternary complexes $(C_6F_5)_3B{-}O(H){-}H{-}OH_2$ (IM0) and $(C_6F_5)_3B{-}O(H){-}H{-}O{=}CR^1R^2$ (IM1-x) are mostly the main initial complexes, and the binary complexes $(C_6F_5)_3B{-}O{=}CR^1R^2$ (IM2-x) and $(C_6F_5)_3B{-}OH_2$ (see Table S1) are secondly. For comparison with different carbonyl compounds and mechanisms, the Gibbs free energy of IM0 is selected as the zero point. In the main manuscript, the transfer hydrogenation pathways of PhCHO and the H_2 generation process are described in detail, while the corresponding Gibbs free energy barriers of other aldehyde/ketone transfer hydrogenations (**1b–i**) are briefly presented for comparison.

3.1. Transfer Hydrogenation of Aldehydes/Ketones (Paths A, B1, B2, C1 and C2). *3.1.1. Computational Data of PhCHO (**1a**). 3.1.1.1. Path A.* As shown in Scheme 7, Figure 1, and Table 1, a $B(C_6F_5)_3$-catalyzed concerted process may proceed via the transition state A-TS-a, delivering $PhCH_2OH$ and $PhSiH_2OH$. The activation Gibbs free energy barrier related to A-TS-a is 31.3 kcal/mol. In A-TS-a, the interatomic distance of the O2–H1 bond is 1.00 Å, implying that the O2–H1 bond is already established, which is attributed to the strong acidity of $(C_6F_5)_3B{-}OH_2$; the angle H2–Si–O1 is 84.5°, and Si has a distorted-trigonal-bipyramidal structure. The vibrational mode of the only imaginary frequency of A-TS-a corresponds to the transfer of H2 from Si to C1, the approach of Si to O1, and the slight shortening of O2–H1. Obviously, Path A is not probable at the working temperature due to the high barrier of A-TS-a.

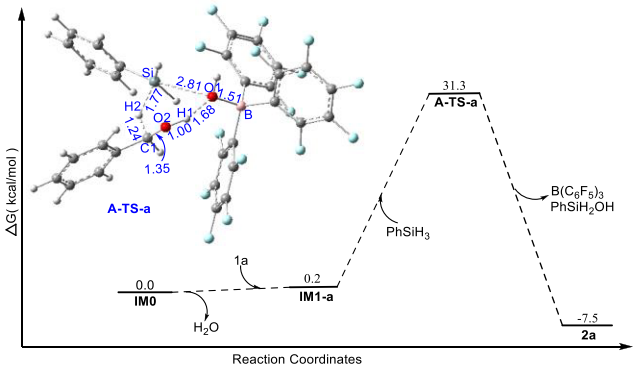

Figure 1. Gibbs free energy profile of Path A for the title reaction related to **1a** in chloroform, with some selected interatomic distances in the inset structure of A-TS-a (energies in kcal/mol, distances in angstroms).

3.1.1.2. Paths B1 and B2. As shown in Scheme 7, Paths B1 and B2 involve siloxane $R^1R^2CH{-}OSiH_2Ph$ formation and subsequent common hydrolysis desilylation steps.

(i) Siloxane $PhCH_2{-}OSiH_2Ph$ generation step(s). As shown in Figure 2 and Table 1, in Path B1, $PhSiH_3$ reacts with the complex $PhHC{=}O{-}B(C_6F_5)_3$ (IM2-a) via B-TS1-a, directly giving $PhCH_2{-}OSiH_2Ph$, and the activation Gibbs free energy barrier is 30.2 kcal/mol. The vibrational mode of the only imaginary frequency of B-TS1-a corresponds to the transfer of H2 from Si to C1 and the approach of Si to O2. The angle H2–Si–O2 in B-TS1-a is 55.2°, this is still a distorted-trigonal-bipyramidal structure.

In Path B2, the Piers S_N2-Si process between PhCHO, $PhSiH_3$ and $B(C_6F_5)_3$ proceeds firstly via B-TS2-a, giving $PhHC{=}O{-}SiH_2Ph^+$ and $(C_6F_5)_3B{-}H^-$, with the activation Gibbs free energy barrier of 17.3 kcal/mol (if the reaction is performed with the stepwise method, this step proceeds under anhydrous conditions, the barrier of B-TS2-a is 12.2 kcal/mol, using IM2-a as the initial point; see Figure 2). The vibrational mode of the only imaginary frequency of B-TS2-a corresponds to the transfer of H2 from Si to B and the approach of Si to O2. The angle H2–Si–O2 in B-TS2-a is 125.9°, the Si center takes a distorted-trigonal-bipyramidal structure. This hypervalent silicon structure may stabilize the transition state, resulting in a lower barrier,[57−59] and that is why the barrier of this S_N2 step is lower. B-IM3-a is a complex of $[PhHC{=}OSiH_2Ph]^+$ and $(C_6F_5)_3B{-}H^-$. The angle H2–Si–O2 in B-IM3-a is 169.5°; here Si takes a typical trigonal-bipyramidal structure. B-IM4-a is another complex of $[PhHC{=}OSiH_2Ph]^+$ and $(C_6F_5)_3B{-}H^-$, ready for the subsequent H^- transfer to C1. And then H^- transfers from $(C_6F_5)_3B{-}H^-$ to carbonyl C by B-TS3-a, delivering siloxane $PhCH_2{-}OSiH_2Ph$ with simultaneous regeneration of $B(C_6F_5)_3$. The activation Gibbs free energy barrier related to B-TS3-a is 2.9 kcal/mol. The vibrational mode of the only imaginary frequency of B-TS3-a corresponds to the transfer of H2 from B to C1.

For $PhCH_2{-}OSiH_2Ph$ formation steps, the barriers of B-TS2-a (17.3 kcal/mol) and B-TS3-a (2.9 kcal/mol) in Path B2 are all evidently lower than that of B-TS1-a (30.2 kcal/mol) in Path B1. So, for the hydrosilylation of carbonyl, the Piers S_N2-Si silane activation mechanism is much more favorable than the carbonyl activation one; this is consistent with the results of Piers, Sakata, et al.[6]

(ii) Hydrolysis desilylation step of $PhCH_2{-}OSiH_2Ph$ common in Paths B1 and B2. Subsequently, as shown in Scheme 7 and Figure 2, the hydrolysis desilylation step of $PhCH_2{-}OSiH_2Ph$ proceeds via B-TS4-a or B-TS5-a, producing $PhCH_2OH$ and $PhSiH_2OH$. The activation Gibbs free energy barriers related to B-TS4-a and B-TS5-a are 22.9 and 30.7 kcal/mol, respectively. The vibrational mode of the only

Table 1. Total Steps and Corresponding Gibbs Free Energy Barriers in Chloroform of Title Reaction Related to 1a in Paths A, B1, B2, C1 and C2 (in kcal mol^{-1})[a]

	TSs (imaginary frequency in i cm^{-1})/$\Delta G^{\ddagger}$		
path			
Path A	A-TS-a (67.01)/31.3		
Path B1	B-TS1-a (204.40)/30.2		B-TS4-a (998.23)/22.9
Path B2	B-TS2-a (42.07)/17.3	B-TS3-a (15.24)/2.9	B-TS4-a (998.23)/22.9
Path C1	C-TS1-a (190.44)/15.4	C-TS2-a (35.67)/14.5	C-TS3-a (73.45)/5.6
Path C2	C-TS1-a (190.44)/15.4	C-TS2-a (33.67)/14.5	C-TS4-a (208.95)/22.6

[a]Respective imaginary frequency of any TS in parentheses.

https://doi.org/10.1021/acsomega.3c05388
ACS Omega 2024, 9, 341−350

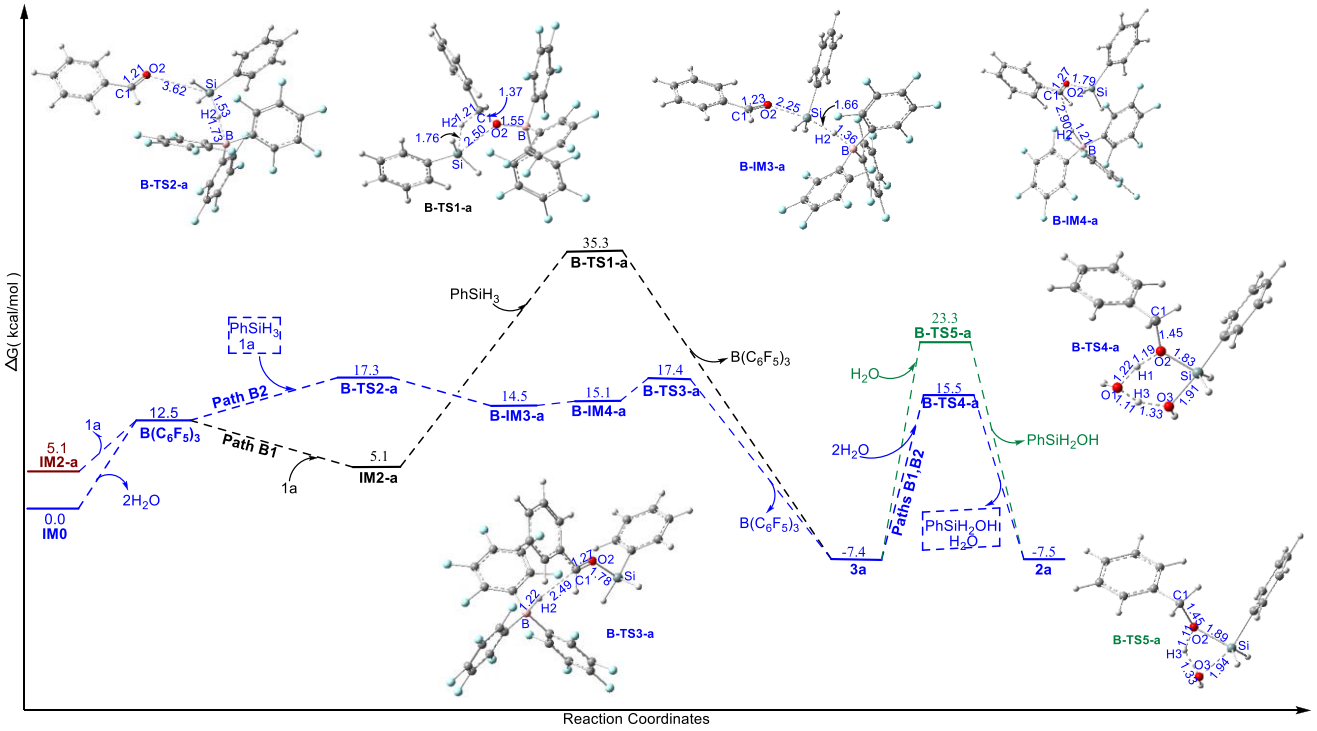

Figure 2. Gibbs free energy profiles of Paths B1 and B2 for the title reaction related to **1a** in chloroform, with some selected interatomic distances in the inset structures (energy in kcal/mol, distance in angstroms).

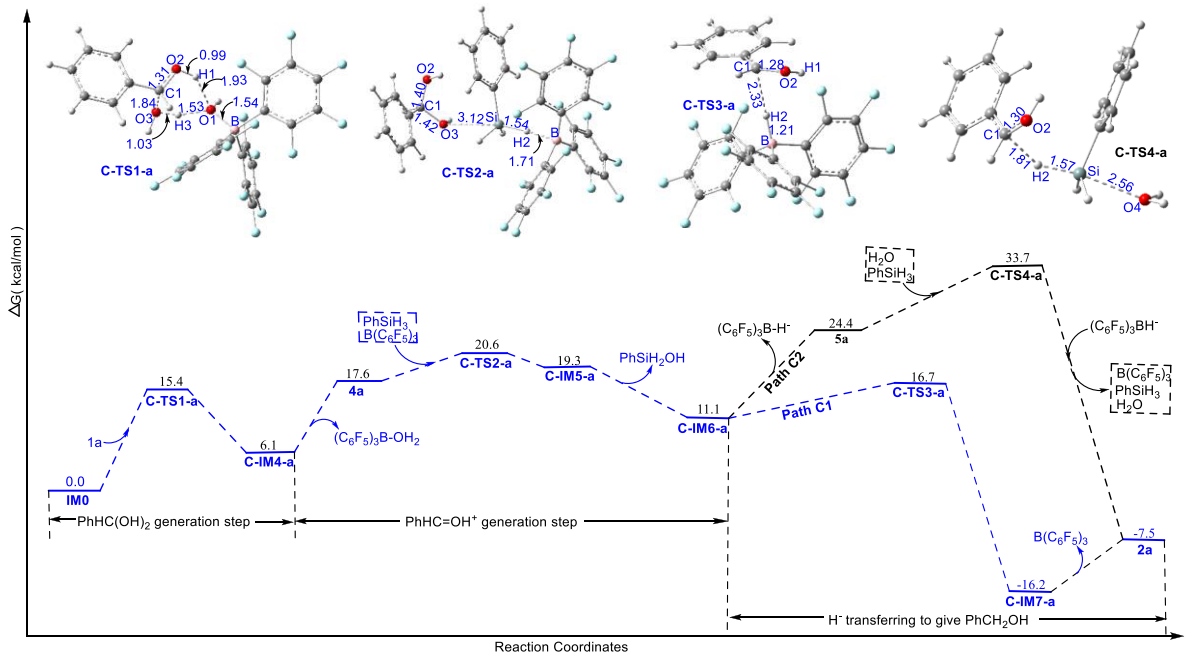

Figure 3. Gibbs free energy profiles of Paths C1 and C2 for the title reaction related to **1a** in chloroform, with some selected interatomic distances in the inset structures (energy in kcal/mol, distance in angstroms).

imaginary frequency of B-TS4-a corresponds to the transfers of H1 from O1 to O2 and of H3 from O1 to O3, with O3 approaching Si, and the breaking of the Si−O2 bond. The only imaginary frequency of B-TS5-a is 813.32 i cm^{-1}, its vibrational mode corresponds to the transfer of H3 from O3 to O2, O3 approaching to Si, and the breaking of the Si−O2 bond. The higher strain of the four-membered-ring transition state B-TS5-a results in its barrier being higher than that of B-TS4-a. So, the hydrolysis desilylation step of $PhCH_2-OSiH_2Ph$ would dominantly proceed by the hexatomic ring transition B-TS4-a. We do not label the pathways involving B-TS5-a, and in the following study for **1b−i**, B-TS5-x will be omitted.

Consequently, Path B2 is one possible pathway with the final hydrolysis desilylation step (B-TS4-a) as the rate-determining step, while Path B1 is not probable at the working temperature

https://doi.org/10.1021/acsomega.3c05388
ACS Omega 2024, 9, 341−350

for the high barrier of the rate-determining step related to B-TS1-a.

3.1.1.3. Paths C1 and C2. There is an equilibrium between aldehydes/ketones and the corresponding geminal diols in aqueous solution, Bernskoetter et al. determined that a concerted addition of 2 water molecules to formaldehyde generates methanediol, by a six-membered-ring transition state,[7] probably some mechanisms such as Paths C1 and C2 (see in Scheme 7) involving geminal diol should be investigated.

(i) Geminal diol $PhHC(OH)_2$ producing step. As shown in Scheme 7, Figure 3, and Table 1, a $B(C_6F_5)_3$-catalyzed concerted addition of $2H_2O$ to carbonyl of PhCHO may proceed via the six-membered-ring transition state C-TS1-a, giving the intermediate geminal diol $PhHC(OH)_2$. C-TS1-a may be regarded as relating to the reaction of PhCHO and IM0, or $1H_2O$ and IM1-a, the initial dominant complexes IM0 and IM1-a are dynamically favorable for this step. The activation Gibbs free energy barrier related to C-TS1-a is 15.4 kcal/mol. Similar to A-TS-a, the O2−H1 distance is 0.99 Å in C-TS1-a, implying that the O2−H1 bond is already established, attributed to the strong acidity of $(C_6F_5)_3B-OH_2$. The vibrational mode of the only imaginary frequency of C-TS1-a corresponds to the approaching of O3 to C1, the transfer of H3 from O3 to O1, the elongation of C1−O2, and slight shortening of O2−H1. C-IM4-a is a complex of $PhHC(OH)_2$ and $(C_6F_5)_3B-OH_2$. In this step, 1 equiv water is consumed, and $(C_6F_5)_3B-OH_2$ has been regenerated in C-IM4-a, so more than 1 equiv water over PhCHO is necessary.

Similarly, the product $PhCH_2OH$ may catalyze the $PhHC(OH)_2$ formation step, instead of one H_2O in C-TS1-a. As shown in Scheme S2, PhCHO may be turned into geminal diol **4a**, by the concerted six-membered-ring transition state C-TS1′-a, with an activation Gibbs free energy barrier of 18.6 kcal/mol, which is obviously higher than that of C-TS1-a (15.4 kcal/mol), and the amount of water is absolutely predominant over $PhCH_2OH$ in the initial phase, so the $PhCH_2OH$ participating in the geminal diol generation process is secondary and negligible.

(ii) $PhHC{=}OH^+$ and $(C_6F_5)_3B-H^-$ formation step. As shown in Scheme 7, Figure 3, and Table 1, another S_N2-Si step between $PhHC(OH)_2$, $PhSiH_3$ and $B(C_6F_5)_3$ proceeds by C-TS2-a, giving $PhHC{=}OH^+$, $(C_6F_5)_3B-H^-$ and $PhSiH_2OH$. The vibrational mode of the only imaginary frequency of C-TS2-a corresponds to the transfer of H2 from Si to B, Si approach to O3, and the breaking of the C1−O3 bond. In C-TS2-a, the angle H2−Si−O3 in C-TS2-a is 167.4° and the Si center takes a typical trigonal-bipyramidal structure, which stabilized the transition state.[57−59] The barrier of this S_N2 step (14.5 kcal/mol related to C-TS2-a) is lower than that of B-TS2-a (17.3 kcal/mol), attributed to greater nucleophilicity of the geminal diol than that of PhCHO. Greater nucleophilicity of the nucleophile, closer to a complete trigonal-bipyramidal Si center in the transition state, would result in a lower barrier. The angle H2−Si−O3 in C-IM5-a is 166.7°, Si takes a typical trigonal-bipyramidal structure. C-IM6-a is the complex of $PhHC{=}OH^+$ and $(C_6F_5)_3B-H^-$ containing the hydrogen bond O2−H1−H2−B.

(iii) H^- transfer to $PhHC{=}OH^+$ to produce $PhCH_2OH$. In Path C1 (see Figure 3 and Table 1), $(C_6F_5)_3B-H^-$ gives H^- to $PhHC{=}OH^+$ via C-TS3-a, producing $PhCH_2OH$ with simultaneous regeneration of $B(C_6F_5)_3$. The vibrational mode of the only imaginary frequency of C-TS3-a corresponds to the leaving of H2 from H1, H2 approaching to C1, and the breaking of B−H2. The activation Gibbs free energy barrier of C-TS3-a is 5.6 kcal/mol.

Path C1 is another possible pathway, in which the first addition step generating $PhHC(OH)_2$ and the second S_N2-Si dehydroxylation step of $PhHC(OH)_2$ giving $PhHC{=}OH^+$ and $(C_6F_5)_3B-H^-$ are partially rate-determining due to their close barriers (15.4 and 14.5 kcal/mol for C-TS1-a and C-TS2-a, respectively).

In Path C2 (see Figure 3 and Table 2), $PhSiH_3$ gives a H^- to $PhHC{=}OH^+$, with H_2O assistance via C-TS4-a, giving $PhCH_2OH$ and $PhSiH_2^+-OH_2$. The activation Gibbs free energy barrier related to C-TS4-a is 22.6 kcal/mol. The vibrational mode of the only imaginary frequency of C-TS4-a corresponds to the transfer of H2 from Si to C1 and the approach of O4 to Si. And finally, $(C_6F_5)_3B-H^-$ gives H^- to $PhSiH_2^+-OH_2$ without any barrier, with $B(C_6F_5)_3$, $PhSiH_3$ and water being regenerated.

Obviously, the transfer of H^- from $(C_6F_5)_3B-H^-$ to $PhHC{=}OH^+$ should be dominant, rather than that from $PhSiH_3$, for the very low barrier of C-TS3-a (5.6 kcal/mol) and the significant barrier of C-TS4-a (22.6 kcal/mol). Path C2 is a possible pathway, with the final H^- transfer step being rate-determining.

So, as shown in Figures 2 and 3 and Table 1, Paths B2, C1, and C2 are possible pathways for the transfer hydrogenation of **1a**. While undoubtedly, Path C1 is dominant, due to the low barriers of C-TS1-a, C-TS2-a and C-TS3-a (15.4, 14.5 and 5.6 kcal/mol, respectively), and the higher barriers of B-TS4-a (22.9 kcal/mol) and C-TS4-a (22.6 kcal/mol). In Path C1, more than 1 equiv water over PhCHO is needed to trigger the reaction.

*3.1.2. Computational Data of **1b−i**.* Figures S2−S4 are the Gibbs free energy profiles of Paths A, B1 and B2, C1 and C2, respectively, related to **1b−i**. B-TS3-c/d does not exist, as verified by potential surface scanning (Figure S5). The corresponding Gibbs free energy barrier of any elementary reaction is shown in Tables 2 and 3.

The following points are detailed in Tables 1−3.

(1) Paths A and B1 are not probable at the working temperature for **1a−i**, due to the high barriers of A-TS-x and B-TS1-x.

Table 2. Gibbs Free Energy Barrier of Any Elementary Reaction in Paths A, B1 and B2 related to 1b−i in Chloroform (in kcal/mol)[a]

		3x generation step(s)			hydrolysis desilylation
	Path A	Path B1	Path B2	Path B2	Paths B1and B2
1x	A-TS-x	B-TS1-x	B-TS2-x	B-TS3-x	B-TS4-x
1b	31.2	29.3	17.4	3.1	23.3
1c	30.1	28.6	18.1	*a*	21.8
1d	26.7	28.2	16.3	*a*	23.1
1e	34.1	38.2	17.7	2.8	22.4
1f	33.9	37.5	17.4	3.4	23.0
1g	31.2	33.5	16.6	3.3	22.1
1h	33.2	39.4	16.7	5.3	22.9
1i	30.4	35.9	16.8	11.5	22.4

[a]No transition state exists.

https://doi.org/10.1021/acsomega.3c05388
ACS Omega 2024, 9, 341−350

Table 3. Gibbs Free Energy Barrier of Any Elementary Reaction in Paths C1 and C2 Related to 1b−i in Chloroform (in kcal mol^{-1})

	steps			
	$R^1R^2C(OH)_2$ generation	$R^1R^2C{=}OH^+$ generation	H^- transfer from $(C_6F_5)_3B{-}H^-$	H^- transfer from $PhSiH_3$
1x	C-TS1-x	C-TS2-x	C-TS3-x	C-TS4-x
1b	16.1	14.9	5.6	22.8
1c	16.4	14.7	1.0	22.3
1d	13.1	15.0	8.4	25.1
1e	15.6	13.8	6.6	25.4
1f	15.9	15.2	6.2	25.7
1g	15.6	15.1	7.1	25.9
1h	25.4	12.8	6.4	27.3
1i	23.3	15.1	6.8	29.0

(2) The electron-withdrawing/donating groups on the substituent group bonding to carbonyl C influence the barriers slightly.

(3) Similar to **1a**, there are three possible pathways (Paths B2, C1 and C2) for aryl/alkyl aldehydes, dialkyl ketones, and alkyl aryl ketones (**1b−g**). Path C1 is dominant, in which the first addition step of $2H_2O$ to carbonyl (C-TS1-x) and subsequent S_N2-Si dehydroxylation step (C-TS2-x) of $R^1R^2C(OH)_2$ are partially rate-determining. More than 1 equiv water over aldehyde/ketone is necessary to trigger Path C1.

(4) For diaryl ketones **1h** and **1i**, the barriers of C-TS4-h (27.3 kcal/mol) and C-TS4-i (29.0 kcal/mol) are higher than those of C-TS4-a−g, attributed to the electron-donating effect and the steric hindrance of two aryls on carbonyl C; this means that Path C2 can be neglected. And the barriers related to C-TS1-h (25.4 kcal/mol) and C-TS1-i (23.3 kcal/mol) are evidently higher than those for C-TS1-a−g, for the electron-donating and steric effect of two aryls on carbonyl C. While the barrier related to C-TS1-i is slightly lower than that of C-TS1-h, due to the strong electron-withdrawing F on one phenyl of **1i**. Consequently, Paths B2 and C1 are competitive for the transfer hydrogenation of **1h** and **1i**, with the steps related to B-TS4-h/i and C-TS1-h/i being respectively rate-determining. At room temperature, Paths B2 and C1 for **1h/i** can hardly happen due to the significant barriers of B-TS4-h/i and C-TS1-h/i. If there were no other competitive reaction, **1h** and **1i** would be effectively reduced into the respective alcohols, when the reaction temperature is appropriately increased.

3.2. The H_2 Generation Process (Path H0). As shown in Scheme 8, Figure 4, and Table 4, a S_N2 process between H_2O, $PhSiH_3$ and $B(C_6F_5)$ proceeds via H-TS1 first, producing the complex H-IM1 of $B(C_6F_5)H^-$ and $PhH_2Si^+{-}OH_2$. The Gibbs free barrier related to H-TS1 is 16.0 kcal/mol, which includes getting free $B(C_6F_5)$ (12.5 kcal/mol) and free $B(C_6F_5)$-catalyzed Si−H activation (3.5 kcal/mol). The dominant initial ternary complexes IM0 and IM1-x increase the barrier of H-TS1 tremendously, relative to that from free $B(C_6F_5)$, $PhSiH_3$ and H_2O. The vibrational mode of the only imaginary frequency of H-TS1 corresponds to the transfer of H2 from Si to B and the approach of Si to O1. Once H-IM1 gains significant dissociation energy (17.8 kcal/mol), free $B(C_6F_5)$-H^- and $PhH_2Si^+{-}OH_2$ are obtained. Subsequently another complex H-IM2 of $B(C_6F_5)H^-$ and $PhH_2Si^+{-}OH_2$ formed. Finally, H_2 is produced via H-TS2, with a very low barrier of 1.2 kcal/mol. The vibrational mode of the only imaginary frequency of H-TS2 corresponds to the formation of H1−H2 and Si−O1 bonds and the breaking of O1−H1 and B−H2 bonds. So, H_2 may be produced along Path H0, in which the step related to H-TS1 (16.0 kcal/mol) and the dissociation of H-IM1 (17.8 kcal/mol) are partially rate-determining, and free $B(C_6F_5)$ and the dissociation of H-IM1 are important.

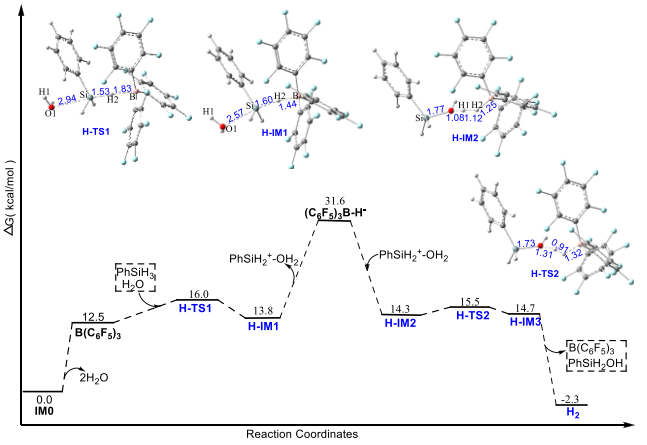

Figure 4. Gibbs free energy profile of Path H0 in chloroform, with some selected interatomic distances in the inset structures (energy in kcal/mol, distance in angstroms).

3.3. Hydrogenation of Aldehydes/Ketones (Paths H1 and H2). Taking **1a** as an example of aldehydes/ketones, as shown in Scheme 8, Figure S6, and Table 4, in Path H1, $B(C_6F_5)_3$ and **1a** behave as FLP to activate H_2, via the transition state H-TS3-a, with a barrier of 30.4 kcal/mol, forming the complex C-IM6. The only imaginary frequency of H-TS3-a corresponds to the heterolysis of H1−H2, and the formation of H1−O2 and B−H2 bonds. In Path H2, $B(C_6F_5)_3$ and the geminal diol **4a** behave as FLP to activate H_2, by the transition state H-TS4-a, with a barrier of 30.3 kcal/mol. The only imaginary frequency of H-TS4-a corresponds to the breaking of H1−H2 and C1−O2 bonds and the formation of H1−O2 and B−H2 bonds. H-IM4-a is the complex of $B(C_6F_5)H^-$, H_2O and $PhHC{=}OH^+$; C-IM6 is formed when H_2O is released. The final step is common to that of Path C1. Obviously, H−H activation is much more difficult than that of Si−H, as determined by the barriers (17.3 kcal/mol of B-TS2-a vs 30.4 kcal/mol of H-TS3-a, 14.5 kcal/mol of C-TS2-a vs 30.3 kcal/mol of H-TS4-a). Similarly, as shown in Figure S6, the barriers related to H-TS3-h/i and TS4-h/i are also about 30 kcal/mol. Therefore, one can say the hydrogenation of aldehydes/ketones is not probable under the working conditions for the higher barriers of H−H activation (H-TS3-x and H-TS4-x). And if H_2 is produced, it would escape from the solution, for there is no reaction consuming it fast enough.

3.4. Competitive Behaviors between the H_2 Generation Process (Path H0) and the Transfer Hydrogenation Pathways (Paths B2 and C1). For the moderate barrier of H-TS1 (16.0 kcal/mol) and the significant dissociation of H-IM1 (17.8 kcal/mol), the H_2 generation process (Path H0) would participate in the competition with the possible transfer hydrogenation pathways. The following

https://doi.org/10.1021/acsomega.3c05388
ACS Omega 2024, 9, 341−350

Table 4. Total Steps and Corresponding Gibbs Free Energy Barriers of Paths H0−2 for H_2 Generation and the Hydrogenation of 1a in Chloroform (in kcal mol^{-1})[a]

Path	TSs (imaginary frequency in i cm^{-1})/$\Delta G^{\ddagger}$		
Path H0	H-TS1 (57.95)/16.0	[H-IM1/17.8][b]	H-TS2 (547.41)/1.2
Path H1	H-TS3-a (412.41)/30.4		C-TS3-a (73.45)/5.6
Path H2	C-TS1-a (190.44)/15.4	H-TS4-a (546.58)/30.3	C-TS3-a (73.45)/5.6

[a]Respective imaginary frequency of any TS in parentheses. [b]intermediate/dissociation energy.

points are detailed in Tables 1−4, Figures 2−4 and Figures S3 and S4.

(i) For **1a−g**, Path C1 is the dominant transfer hydrogenation pathway. The barriers of C-TS1-x, C-TS2-x, and C-TS3-x (13.1−16.4, 13.8−15.2 and 1.0−8.4 kcal/mol, respectively) are all obviously lower than the dissociation energy of H-IM1 (17.8 kcal/mol) and mostly lower than the barrier of H-TS1(16.0 kcal/mol); moreover, the complexes C-IM7-x are located at very low positions on the energy profiles (Figure 3 and Figure S4). Moreover, the initial dominant complexes IM0 and IM1-x are dynamically favorable for Path C1 and disadvantageous for Path H0. Path C1 to produce **2a−g** is dominant over the above H_2 generation process Path H0. H-IM1 would prefer to come back to free $B(C_6F_5)_3$, $PhSiH_3$ and H_2O by a barrier of 2.2 kcal/mol and then to form IM0 and IM1-x, ready for Path C1, rather than the dissociation with a significant energy demand (17.8 kcal/mol). So, H_2 is hardly produced in **1a−g** reaction systems at the working temperature, and **1a−g** can be reduced into alcohols chemoselectively and effectively, which is consistent with our experiments.[48]

(ii) For **1h/i**, Paths B2 and C1 are competitive transfer hydrogenation pathways. Due to the higher barriers of C-TS1-h/i (25.4 and 23.3 kcal/mol, respectively) and B-TS4-h/i (22.9 and 22.4 kcal/mol, respectively), Paths B2 and C1 have no competitive advantage over Path H0. **3h/i** are located at lower positions on the Gibbs free energy profiles (Figure 2 and Figure S3) of Path B2, the barriers of B-TS3-h/ are very low (3.5 or 7.3 kcal/mol), and the barriers of B-TS2-h/i (16.7 or 16.8 kcal/mol) are slightly higher than that of H-TS1 (16.0 kcal/mol) and slightly lower than the dissociation energy of H-IM1 (17.8 kcal/mol). The process of **3h/i** generation along Path B2 should compete with Path H0. There are two non-negligible barriers in Path H0 (16.0 and 17.8 kcal/mol), and the initial dominant complexes IM0 and IM1-x decrease the amount of free $B(C_6F_5)_3$; the evolution of H_2 must be slow, which is consistent with our experiments at room temperature. When increasing the reaction temperature to ∼90 °C, the reactions of Paths B2 and C1 can proceed; nevertheless, the reaction rate of Path H0 is increased, which would consume H_2O rapidly, and also partial H_2O is evaporated out of the solution, so only small amounts of **3h/i** and **2h/i** may be produced. Because of the competitive advantage of Path H0 over Paths B2 and C1, **1h/i** cannot be efficiently reduced into the respective alcohols using the one-time feeding one-pot method.

4. CONCLUSION

(i) For the stepwise method, Path B2 is the only mechanism, and herein the barriers of B-TS2-x should be calculated relative to the adducts $R^1R^2C{=}O{-}B(C_6F_5)_3$ for the anhydrous conditions.

(ii) For aryl/alkyl aldehydes, dialkyl ketones, and alkyl aryl ketones (**1a−g**), the one-time feeding one-pot method is suggested. Path C1 is first determined as the dominant transfer hydrogenation pathway, in which the first addition step of $2H_2O$ to carbonyl (C-TS1-x) and subsequent S_N2-Si dehydroxylation step (C-TS2-x) of $R^1R^2C(OH)_2$ are partially rate-determining. And Path C1 to produce **2a−g** is dominant over the H_2 generation process Path H0. The H_2 generation is efficiently inhibited by the competitive advantage of Path C1. Moreover, the initial dominant existence of the complexes IM0 and IM1-x is dynamically favorable for Path C1 and disadvantageous for Path H0. H_2 is hardly produced in **1a−g** reaction systems at the working temperature, and **1a−g** can be reduced into alcohols chemoselectively and effectively; more than 1 equiv water over the substrates is necessary to trigger the title reaction, which is consistent with the experiments.

(iii) For diaryl ketones (**1h/i**), the one-time feeding one-pot method is not suggested. Paths B2 and C1 are competitive pathways for transfer hydrogenation of **1h/i**, but Paths B2 and C1 have no competitive advantage with Path H0 for H_2 generation. The processes of **3h/i** generation along Path B2 and the H_2 generation (Path H0) are competitive, and the **3h/i** generation process has a slight competitive advantage over Path H0, due to the moderate barrier of H-TS1 and the significant dissociation energy of H-IM1 in Path H0, and the dominant existence of IM0 and IM1-x results in the absence of free $B(C_6F_5)_3$, so the evolution of H_2 is slow at room temperature. Increasing the reaction temperature is more favorable for H_2 evolution, rather than **2h/i** production.

■ ASSOCIATED CONTENT

Supporting Information

The Supporting Information is available free of charge at https://pubs.acs.org/doi/10.1021/acsomega.3c05388.

Potential surface scanning, Gibbs free energy profiles of Paths A, B1, B2, C1, C2, H1 and H2, optimized geometries, Gibbs free energy changes of binary and ternary complex formation, addition of $1H_2O$ and $1PhCH_2OH$ to **1a**, and the optimized Cartesian coordinates (PDF)

■ AUTHOR INFORMATION

Corresponding Authors

Yunqing He − *Sichuan Province Engineering Technology Research Center of Oil Cinnamon and Key Lab of Process Analysis and Control of Sichuan Universities, Yibin University, Yibin 644000 Sichuan, People's Republic of*

https://doi.org/10.1021/acsomega.3c05388
ACS Omega 2024, 9, 341−350

China; orcid.org/0000-0002-6764-4463; Email: yunqing0228@163.com

Wanli Nie − *Department of Material Science, Shenzhen MSU-BIT University, Shenzhen 518172 Guangdong, People's Republic of China*; orcid.org/0000-0001-8851-0002; Email: niewl126@126.com

Authors

Zhiguo Wen − *Leshan Engineering Research Center for Medicinal Components of Characteristic AgroProducts and Leshan West Silicon Materials Photovoltaic and New Energy Industry Technology research Institute, Leshan Normal University, Leshan 614000 Sichuan, People's Republic of China*; orcid.org/0000-0002-9736-3937

Li Yang − *Faculty of Materials and Chemical Engineering, Yibin University, Yibin 644000 Sichuan, People's Republic of China*

Complete contact information is available at: https://pubs.acs.org/10.1021/acsomega.3c05388

Author Contributions

[▽]Y.H. and W.N. contributed equally.

Author Contributions

The manuscript was written through contributions of all authors. All authors have given approval to the final version of the manuscript.

Notes

The authors declare no competing financial interest.

■ ACKNOWLEDGMENTS

This study was financially supported by the National Natural Science Foundation of China (No. 21542011), the Startup Project supported by Yibin University (No. 2021QH03, 2020QH09), the Key Lab of Process Analysis and Control of Sichuan Universities (No. GCFX2021004), and the Sichuan Province Engineering Technology Research Center of Oil Cinnamon (No. 22YZZ06, 21YZZ01).

■ REFERENCES

(1) de Vries, J. G.; Elsevier, C. J. *The Handbook of Homogeneous Hydrogenation*; Wiley-VCH: 2008.

(2) Volkov, A.; Gustafson, K. P. J.; Tai, C. W.; Verho, O.; Baeckvall, J. E.; Adolfsson, H. Mild Deoxygenation of Aromatic Ketones and Aldehydes over Pd/C Using Polymethylhydrosiloxane as the Reducing Agent. *Angew. Chem., Int. Ed.* **2015**, *54*, 5122−5126.

(3) Guo, J.; Chen, J.; Lu, Z. Cobalt-catalyzed asymmetric hydroboration of aryl ketones with pinacolborane. *Chem. Commun.* **2015**, *51*, 5725−5727.

(4) Chakraborty, S.; Bhattacharya, P.; Dai, H.; Guan, H. Nickel and Iron Pincer Complexes as Catalysts for the Reduction of Carbonyl Compounds. *Acc. Chem. Res.* **2015**, *48*, 1995−2003.

(5) Chakraborty, S.; Lagaditis, P. O.; Förster, M.; Bielinski, E. A.; Hazari, N.; Holthausen, M. C.; Jones, W. D.; Schneider, S. Well-Defined Iron Catalysts for the Acceptorless Reversible Dehydrogenation-Hydrogenation of Alcohols and Ketones. *ACS Catal.* **2014**, *4*, 3994−4003.

(6) Zeng, G.; Sakaki, S.; Fujita, K.; Sano, H.; Yamaguchi, R. Efficient Catalyst for Acceptorless Alcohol Dehydrogenation: Interplay of Theoretical and Experimental Studies. *ACS Catal.* **2014**, *4*, 1010−1020.

(7) Bielinski, E. A.; Förster, M.; Zhang, Y.; Bernskoetter, W. H.; Hazari, N.; Holthausen, M. C. Base-Free Methanol Dehydrogenation Using a Pincer-Supported Iron Compound and Lewis Acid Co-catalyst. *ACS Catal.* **2015**, *5*, 2404−2415.

(8) Zhang, J.; Qu, L.; Shi, G.; Liu, J.; Chen, J.; Dai, L. N,P-Codoped Carbon Networks as Efficient Metal-free Bifunctional Catalysts for Oxygen Reduction and Hydrogen Evolution Reactions. *Angew. Chem.* **2016**, *128*, 2270−2274.

(9) Welch, G. C.; San Juan, R. R.; Masuda, J. D.; Stephan, D. W. Reversible, Metal-Free Hydrogen Activation. *Science* **2006**, *314*, 1124−1126.

(10) Chase, P. A.; Welch, G. C.; Jurca, T.; Stephan, D. W. Metal-Free Catalytic Hydrogenation. *Angew. Chem.* **2007**, *119*, 8196−8199.

(11) Welch, G. C.; Stephan, D. W. Facile Heterolytic Cleavage of Dihydrogen by Phosphines and Boranes. *J. Am. Chem. Soc.* **2007**, *129*, 1880−1881.

(12) Spies, P.; Schwendemann, S.; Lange, S.; Kehr, G.; Fröhlich, R.; Erker, G. Metal-Free Catalytic Hydrogenation of Enamines, Imines, and Conjugated Phosphinoalkenylboranes. Angew. *Chem. Int. Ed.* **2008**, *47*, 7543−7546.

(13) Stephan, D. W. Frustrated Lewis pairs": a concept for new reactivity and catalysis. *Org. Biomol. Chem.* **2008**, *6*, 1535−1539.

(14) Dai, L.; Xue, Y.; Qu, L.; Choi, H. J.; Baek, J. B. Metal-Free Catalysts for Oxygen Reduction Reaction. *Chem. Rev.* **2015**, *115*, 4823−4892.

(15) Stephan, D. W.; Erker, G. Frustrated Lewis Pairs: Metal-free Hydrogen Activation and More. Angew. *Chem., Int. Ed.* **2010**, *49*, 46−76.

(16) Stephan, D. W.; Erker, G. Frustrated Lewis Pair Chemistry: Development and Perspectives. *Angew. Chem., Int. Ed.* **2015**, *54*, 6400−6441.

(17) Tussing, S.; Greb, L.; Tamke, S.; Schirmer, B.; Muhle-Goll, C.; Luy, B.; Paradies, J. Autoinduced Catalysis and Inverse Equilibrium Isotope Effect in the Frustrated Lewis Pair Catalyzed Hydrogenation of Imines. *Chem. - Eur. J.* **2015**, *21*, 8056−8059.

(18) Tussing, S.; Kaupmees, K.; Paradies, J. Paradies, Structure-Reactivity Relationship in the Frustrated Lewis Pair (FLP)-Catalyzed Hydrogenation of Imines. *Chem. - Eur. J.* **2016**, *22*, 7422−7426.

(19) Rokob, T. A.; Hamza, A.; Stirling, A.; Papai, I. On the Mechanism of $B(C_6F_5)_3$-Catalyzed Direct Hydrogenation of Imines: Inherent and Thermally Induced Frustration. *J. Am. Chem. Soc.* **2009**, *131*, 2029−2036.

(20) Blackwell, J. M.; Sonmor, E. R.; Scoccitti, T.; Piers, W. E. $B(C_6F_5)_3$-Catalyzed Hydrosilation of Imines via Silyliminium Intermediates. *Org. Lett.* **2000**, *2*, 3921−3923.

(21) Chase, P. A.; Jurca, T.; Stephan, D. W. Lewis acid-catalyzed hydrogenation: $B(C_6F_5)_3$-mediated reduction of imines and nitriles with H_2. *Chem. Commun.* **2008**, 1701−1703.

(22) Liu, Y.; Du, H. Frustrated Lewis Pair Catalyzed Asymmetric Hydrogenation. *Acta Chim. Sinica.* **2014**, *72*, 771−777.

(23) Fasano, V.; Ingleson, M. J. Recent Advances in Water-Tolerance in Frustrated Lewis Pair Chemistry. *Synthesis* **2018**, *50*, 1783−1795.

(24) Wang, H.; Yi, Z.; Pan, Z.; Fu, H.; Ling, F.; Zhong, W. Progress of Frustrated Lewis Pairs in Catalytic Hydrogenation. *Chin. J. Org. Chem.* **2017**, *37*, 301−313.

(25) Lindqvist, M.; Sarnela, N.; Sumerin, V.; Chernichenko, K.; Leskela, M.; Repo, T. Heterolytic dihydrogen activation by $B(C_6F_5)_3$ and carbonyl compounds. *Dalton Trans.* **2012**, *41*, 4310−4312.

(26) Longobardi, L. E.; Tang, C.; Stephan, D. W. Stoichiometric reductions of alkyl-substituted ketones and aldehydes to borinic esters. *Dalton Trans.* **2014**, *43*, 15723−15726.

(27) Spies, P.; Erker, G.; Kehr, G.; Bergander, K.; Fraeohlich, R.; Grim-me, S.; Stephan, D. W. Rapid intramolecular heterolytic dihydrogen activation by a four-membered heterocyclic phosphane-borane adduct. *Chem. Commun.* **2007**, *47*, 5072−5074.

(28) Mahdi, T.; Stephan, D. W. Enabling catalytic ketone hydrogenation by frustrated Lewis pairs. *J. Am. Chem. Soc.* **2014**, *136*, 15809−15812.

(29) Scott, D. J.; Fuchter, M. J.; Ashley, A. E. Nonmetal catalyzed hydrogenation of carbonyl compounds. *J. Am. Chem. Soc.* **2014**, *136*, 15813−15816.

(30) Scott, D. J.; Simmons, T. R.; Lawrence, E. J.G.; Wildgoose, G.; Fuchter, M. J.; Ashley, A. E. Facile Protocol for Water-Tolerant "Frustrated Lewis Pair"-Catalyzed Hydrogenation. *ACS Catal.* **2015**, *5*, 5540−5544.
(31) Mahdi, T.; Stephan, D. W. Facile Protocol for Catalytic Frustrated Lewis Pair Hydrogenation and Reductive Deoxygenation of Ketones and Aldehydes. *Angew. Chem., Int. Ed.* **2015**, *54*, 8511−8514.
(32) Li, N.; Zhang, W.-X. Frustrated Lewis Pairs: Discovery and Overviews in Catalysis. *Chin. J. Chem.* **2020**, *38*, 1360−1370.
(33) Parks, D. J.; Piers, W. E. Tris(pentafluorophenyl)boron-Catalyzed Hydrosilation of Aromatic Aldehydes, Ketones, and Esters. *J. Am. Chem. Soc.* **1996**, *118*, 9440−9441.
(34) Sakata, K.; Fujimoto, H. Quantum Chemical Study of $B(C_6F_5)_3$-Catalyzed Hydrosilylation of Carbonyl Group. *J. Org. Chem.* **2013**, *78*, 12505−12512.
(35) Parks, D. J.; Blackwell, J. M.; Piers, W. E. Studies on the Mechanism of $B(C_6F_5)_3$-Catalyzed Hydrosilation of Carbonyl Functions. *J. Org. Chem.* **2000**, *65*, 3090−3098.
(36) Rendler, S.; Oestreich, M. Conclusive Evidence for an S_N2-Si Mechanism in the $B(C_6F_5)_3$-Catalyzed Hydrosilylation of Carbonyl Compounds: Implications for the Related Hydrogenation. *Angew. Chem., Int. Ed.* **2008**, *47*, 5997−6000.
(37) Gyomore, A.; Bakos, M.; Foldes, T.; Papai, I.; Domjan, A.; Soos, T. Moisture-Tolerant Frustrated Lewis Pair Catalyst for Hydrogenation of Aldehydes and Ketones. *ACS Catal.* **2015**, *5*, 5366−5372.
(38) Dorkó, É.; Szabó, M.; Kótai, B.; Pápai, I.; Domján, A.; Soós, T. Expanding the Boundaries of Water-Tolerant Frustrated Lewis Pair Hydrogenation: Enhanced Back Strain in the Lewis Acid Enables the Reductive Amination of Carbonyls. *Angew. Chem., Int. Ed.* **2017**, *56*, 9512−9516.
(39) Fasano, V.; Radcliffe, J. E.; Ingleson, M. J. $B(C_6F_5)_3$-Catalyzed Reductive Amination using Hydrosilanes. *ACS Catal.* **2016**, *6*, 1793−1798.
(40) Fasano, V.; Ingleson, M. J. Expanding Water/Base Tolerant Frustrated Lewis Pair Chemistry to Alkylamines Enables Broad Scope Reductive Aminations. *Chem. - Eur. J.* **2017**, *23*, 2217−2224.
(41) Kim, E.; Park, S.; Chang, S. Silylative Reductive Amination of α,β-Unsaturated Aldehydes: A Convenient Synthetic Route to β-Silylated Secondary Amines. *Chem. - Eur. J.* **2018**, *24*, 5765−5769.
(42) Chen, H.-C.; Yan, L.-N.; Wei, H.-Y. Mechanism of Boron-Catalyzed N-Alkylation of Primary and Secondary Arylamines with Ketones Using Silanes under "Wet" Conditions. *Organometallics.* **2018**, *37*, 3698−3707.
(43) (a) Yu, Y.; Zhu, Y.; Bhagat, M. N.; Raghuraman, A.; Hirsekorn, K. F.; Notestein, J. M.; Nguyen, S. T.; Broadbelt, L. J. Mechanism of Regioselective Ring-Opening Reactions of 1,2-Epoxyoctane Catalyzed by Tris(pentafluorophenyl)borane: A Combined Experimental, Density Functional Theory, and Microkinetic Study. *ACS Catal.* **2018**, *8*, 11119−11133.
(44) Bhagat, M. N.; Bennett, C. K.; Chang, G.-F.; Zhu, Y.; Raghuraman, A.; Belowich, M. E.; Nguyen, S. T.; Broadbelt, L. J.; Notestein, J. M. Enhancing the Regioselectivity of $B(C_6F_5)_3$-Catalyzed Epoxide Alcoholysis Reactions Using Hydrogen-Bond Acceptors. *ACS Catal.* **2019**, *9*, 9663−9670.
(45) Bennett, C. K.; Bhagat, M. N.; Zhu, Y.; Yu, Y.; Raghuraman, A.; Belowich, M. E.; Nguyen, S. T.; Notestein, J. M.; Broadbelt, L. J. Strong Influence of the Nucleophile on the Rate and Selectivity of 1,2-Epoxyoctane Ring Opening Catalyzed by Tris(pentafluorophenyl)-borane, $B(C_6F_5)_3$. *ACS Catal.* **2019**, *9*, 11589−11602.
(46) He, Y.; Teng, J.; Tian, C.; Borzov, M.; Hu, Q.; Nie, W. Reductive Amination by One Pot Reaction of Aldehydes and Alkoxyamines Catalyzed by $B(C_6F_5)_3$. *Acta Chim. Sinica.* **2018**, *76*, 774−778.
(47) He, Y.; Nie, W.; Xue, Y.; Hu, Q. Mechanistic insight into $B(C_6F_5)_3$ catalyzed imine reduction with $PhSiH_3$ under stoichiometric water conditions. *RSC Adv.* **2021**, *11*, 20961−20969.
(48) Sun, G.; He, Y.; Tian, C.; Borzov, M.; Hu, Q.; Nie, W. $B(C_6F_5)_3$-Catalyzed Chemoselective Reduction of Carbonyl Compounds under Water Conditions. *Acta Chim. Sinica.* **2019**, *77*, 166−171.
(49) Gonzalez, C.; Schlegel, H. B. An improved algorithm for reaction path Following. *J. Chem. Phys.* **1989**, *90*, 2154−2161.
(50) Gonzalez, C.; Schlegel, H. B. Reaction Path Following in Mass-Weighted Internal Coordinates. *J. Phys. Chem.* **1990**, *94*, 5523−5527.
(51) Hehre, W. J.; Ditchfield, R.; Pople, J. A. Self-Consistent Molecular Orbital Methods. XII. Further Extensions of Gaussian-Type Basis Sets for Use in Molecular Orbital Studies of Organic Molecules. *J. Chem. Phys.* **1972**, *56*, 2257−2261.
(52) Grimme, S.; Ehrlich, S.; Goerigk, L. Effect of the Damping Function in Dispersion Corrected Density Functional Theory. *J. Comput. Chem.* **2011**, *32*, 1456−1465.
(53) Miertus, S.; Tomasi, J. Approximate Evaluations of the Electrostatic Free Energy and Internal Energy Changes in Solution Processes. *Chem. Phys.* **1982**, *65*, 239−245.
(54) Cossi, M.; Barone, V.; Cammi, R.; Tomasi, J. Ab initio Study of Solvated Molecules: A New Implementation of the Polarizable Continuum Model. *Chem. Phys. Lett.* **1996**, *255*, 327−335.
(55) Marenich, A. V.; Cramer, C. J.; Truhlar, D. G. Universal Solvation Model Based on Solute Electron Density and on a Continuum Model of the Solvent Defined by the Bulk Dielectric Constant and Atomic Surface Tensions. *J. Phys. Chem. B* **2009**, *113*, 6378−6396.
(56) Frisch, M. J.; Trucks, G. W.; Schlegel, H. B.; Scuseria, G. E.; Robb, M. A.; Cheeseman, J. R.; Scalmani, G.; Barone, V.; Petersson, G. A.; Nakatsuji, H.; Li, X.; Caricato, M.; Marenich, A. V.; Bloino, J.; Janesko, B. G.; Gomperts, R.; Mennucci, B.; Hratchian, H. P.; Ortiz, J. V.; Izmaylov, A. F.; Sonnenberg, J. L.; Williams-Young, D.; Ding, F.; Lipparini, F.; Egidi, F.; Goings, J.; Peng, B.; Petrone, A.; Henderson, T.; Ranasinghe, D.; Zakrzewski, V. G.; Gao, J.; Rega, N.; Zheng, G.; Liang, W.; Hada, M.; Ehara, M.; Toyota, K.; Fukuda, R.; Hasegawa, J.; Ishida, M.; Nakajima, T.; Honda, Y.; Kitao, O.; Nakai, H.; Vreven, T.; Throssell, K.; Montgomery, J. A., Jr.; Peralta, J. E.; Ogliaro, F.; Bearpark, M. J.; Heyd, J. J.; Brothers, E. N.; Kudin, K. N.; Staroverov, V. N.; Keith, T. A.; Kobayashi, R.; Normand, J.; Raghavachari, K.; Rendell, A. P.; Burant, J. C.; Iyengar, S. S.; Tomasi, J.; Cossi, M.; Millam, J. M.; Klene, M.; Adamo, C.; Cammi, R.; Ochterski, J. W.; Martin, R. L.; Morokuma, K.; Farkas, O.; Foresman, J. B.; Fox, D. J. *Gaussian 16, Revision A.03*; Gaussian, Inc.: 2016.
(57) Singh, V.; Sakaki, S.; Deshmukh, M. M. Ni(I)-Hydride Catalyst for Hydrosilylation of Carbon Dioxide and Dihydrogen Generation: Theoretical Prediction and Exploration of Full Catalytic Cycle. *Organometallics.* **2018**, *37*, 1258−1270.
(58) Deshmukh, M. M.; Sakaki, S. Generation of Dihydrogen Molecule and Hydrosilylation of Carbon Dioxide Catalyzed by Zinc Hydride Complex: Theoretical Understanding and Prediction. *Inorg. Chem.* **2014**, *53*, 8485−8493.
(59) Singh, V.; Sakaki, S.; Deshmukh, M. M. Theoretical Prediction of Ni(I)-Catalyst for Hydrosilylation of Pyridine and Quinoline. *J. Comput. Chem.* **2019**, *40*, 2119−2130.

https://doi.org/10.1021/acsomega.3c05388
ACS Omega 2024, 9, 341−350